

1    **Competition constrains parasite adaptation to thermal heterogeneity**

2    **Samuel TE Greenrod<sup>1#</sup>, Daniel Cazares<sup>1</sup>, Weronika Slesak<sup>1</sup>, Tobias E Hector<sup>1</sup>, R. Craig  
3    MacLean<sup>1,2</sup>, Kayla C King<sup>1,3,4,#</sup>**

4    <sup>1</sup> Department of Biology, University of Oxford, Oxford, UK

5    <sup>2</sup> All Souls College, High Street, Oxford OX1 4AL, UK

6    <sup>3</sup> Department of Zoology, University of British Columbia, Vancouver, Canada

7    <sup>4</sup> Department of Microbiology & Immunology, University of British Columbia, Vancouver, Canada

8    <sup>#</sup>Correspondence: [greenrodsam@gmail.com](mailto:greenrodsam@gmail.com) (Samuel Greenrod); [kayla.king@ubc.ca](mailto:kayla.king@ubc.ca) (Kayla King)

9

10    **Abstract**

11    Temporal thermal heterogeneity is expected to favour intermediate, generalist phenotypes  
12    that can maintain growth across a broad thermal range but have sub-optimal growth at any  
13    single temperature. Yet, thermal variation typically occurs in the presence of additional  
14    selection pressures which may interact to constrain adaptation to temperature. We  
15    propagated competing lytic viral parasites (bacteriophages  $\phi$ 14-1 and  $\phi$ LUZ19) of  
16    *Pseudomonas aeruginosa* under fluctuating temperatures (37–42°C) in monoculture and in  
17    co-culture. Without competition, fluctuating temperatures favoured intermediate thermal  
18    phenotypes in the phage  $\phi$ 14-1 and resulted in more variable evolutionary outcomes  
19    compared to static conditions. However, co-selection from fluctuating temperatures and  
20    competition led to restricted thermal adaptation, slower evolutionary rates, and fewer  
21    putative adaptive mutations in the  $\phi$ LUZ19 competitor. Our study highlights the potential for  
22    reduced adaptive capacity in interacting communities amidst global climate change.

23

24    **Key words:** temperature, thermal heterogeneity, competition, evolution, co-selection, phage

25

26    **Introduction**

27    Thermal heterogeneity plays a key role in shaping species' evolutionary trajectories. Spanning  
28    a broad range of timescales, temperatures fluctuate across multi-year periods (ENSO),  
29    between seasons, and even on the order of hours through diurnal (24-hour) cycles. Very slow  
30    or rapid thermal fluctuation frequencies, with respect to generation times, typically lead to  
31    similar adaptation to static environments through selective sweeps by specialist variants  
32    [1,2]. Moderate fluctuation frequencies select for thermal generalists which have  
33    intermediate phenotypes across temperatures [1–3]. Generalist phenotypes often arise  
34    through the acquisition of multiple specialist mutations [4] or single pleiotropic mutations [5].  
35    Thermal heterogeneity can also promote diversifying selection [6–8] leading to the  
36    maintenance of thermal specialist sub-populations [7]. The mechanisms of adaptation to  
37    thermal heterogeneity depend on the fluctuation frequency relative to generation time [9];

38 fluctuations that far exceed generation times in fast-replicating species may favour  
39 specialists, but in slow-replicating species may instead select for generalists.

40 Thermal heterogeneity typically occurs in the context of multiple selective pressures. For  
41 example, warming can impose selection on species that are simultaneously adapting to other  
42 abiotic stressors or to interactions with predators, competitors, or antagonists [10,11]. The  
43 presence of multiple selection pressures can constrain evolution rates through combined  
44 negative effects on species fitness which reduce population sizes and mutational supply  
45 [12,13]. Co-selection can also restrict adaptation through pleiotropic fitness trade-offs; high  
46 fitness under one stressor reduces fitness under another [14,15]. Temporal thermal  
47 heterogeneity is expected to promote genetic diversification by increasing niche differences  
48 [16] and so may offset the diversity-suppressing impacts of co-selection. However, some  
49 studies have indicated that co-selection involving temporal heterogeneity can exacerbate  
50 evolutionary constraint [17–19]. The ability of species to adapt to thermal heterogeneity  
51 amidst other selection pressures plays an important role in the maintenance of global  
52 biodiversity and species extinction risk [12,20–22].

53 Parasites provide an ideal group of organisms to study adaptation to thermal heterogeneity.  
54 Parasites are often exposed to diverse environments and stressors across their multi-stage  
55 life cycles. They can have both free-living, vector-based, and host-associated life stages [23].  
56 By moving through numerous external environments during and between replicative cycles,  
57 parasites experience high temporal thermal heterogeneity (Greenrod et al., in press; [24]).  
58 During the infection stage, parasites can also induce fevers in hosts, driving thermal changes  
59 [25]. Finally, parasites are expected to face increasingly frequent thermal extremes as a result  
60 of global climate change [26]. While contending with variable thermal environments,  
61 parasites must adapt to host immune responses [27] and competition with co-infecting  
62 parasites in the same host population or individual [28]. Within and between-host  
63 competition are primary determinants of parasite virulence [29] signifying that interactions  
64 between competition and environment-based selection can shape parasite evolution [30].

65 We predicted that thermal heterogeneity would select for generalist parasite populations,  
66 which have intermediate phenotypes, and promote genetic diversity [1]. We also predicted  
67 that co-selection with other environmental stressors would constrain parasite adaptation  
68 [17]. We passaged two lytic viral parasites (thermal generalist φLUZ19 and specialist φ14-1)  
69 under a fluctuating thermal regime (37–42°C) in the absence and presence of a phage  
70 competitor. Phages evolved with a static bacterial host, *Pseudomonas aeruginosa*. We  
71 compared populations evolved under fluctuating temperatures concurrently with those  
72 evolved under a static regime (37°C and 42°C), the latter presented in ref. [31]. We evaluated  
73 phage phenotypic adaptation through growth assays at 37°C and 42°C. We also conducted  
74 phage population sequencing to identify adaptive mutations and measure evolutionary rates.

75

76

77

78 **Methods and Materials**

79 **Strains, Storage, and Culture Conditions**

80 This study builds on a previously published experimental framework [31] using the same  
81 bacterial host and bacteriophage strains. *Pseudomonas aeruginosa* PAO1 was used as the  
82 non-evolving bacterial host throughout. Two lytic phages,  $\phi$ Luz19 and  $\phi$ 14-1, were used due  
83 to their known thermal response differences:  $\phi$ Luz19 performs well at both 37°C and 42°C,  
84 while  $\phi$ 14-1 is growth-restricted at 42°C [31,32]. Phage lysates and bacterial stocks were  
85 prepared as in refs [31,32].

86 **Experimental Evolution**

87 The experimental evolution design closely followed that of ref. [31] with additional  
88 treatments incorporating fluctuating temperatures. Phages were serially passaged for 15 days  
89 under four conditions: monoculture and co-culture, each at either static or fluctuating  
90 temperatures (daily shifts between 37°C and 42°C). Each treatment included six independent  
91 replicate populations initiated from a single ancestral lysate.

92 Phages were propagated without shaking with a non-evolving ancestral PAO1 bacterial host.  
93 For the initial passage, ancestral phage lysates were diluted to  $10^8$  PFU/ml and 300 $\mu$ l were  
94 added to 2.7ml  $10^8$  CFU/ml bacterial culture in loose-lid 14ml falcon tubes. Phage co-culture  
95 populations were prepared by combining 150 $\mu$ l each of  $\phi$ Luz19 and  $\phi$ 14-1  $10^8$  PFU/ml lysates  
96 prior to mixing with bacteria. The initial passage phage densities were  $\sim 10^7$  PFU/ml resulting  
97 in a phage/bacteria ratio (multiplicity of infection, MOI) =  $\sim 0.1$ . Following addition of bacterial  
98 cultures, tubes were incubated statically at 37°C or 42°C in circulating water baths for 8h.  
99 Fluctuating passages started and ended at 37°C.

100 After incubation, phage populations were harvested by centrifugation (3,095 $\times g$ , 5 min) to  
101 pellet bacteria, followed by sterile filtration through 0.2 $\mu$ m filters. Filtrates were stored at  
102 4°C. In subsequent passages, 300 $\mu$ l of lysate was transferred into fresh PAO1 cultures.

103 **Phage Quantification**

104 Phage titres were determined via the double-layer overlay method [33] following the same  
105 protocols as in refs [31,32]. Briefly, bacterial lawns were prepared by mixing 10mL of melted  
106 LB-top agar with 300 $\mu$ L of a *P. aeruginosa* PAO1 overnight culture. Phage lysates were serially  
107 diluted, and 10 $\mu$ L was spotted onto the bacterial lawns. After incubating plates for 6–8 h at  
108 37°C, spots with the highest number of discernible plaques were counted and reported.  
109  $\phi$ Luz19- or  $\phi$ 14-1-resistant PAO1 strains were used for selective plating enabling separate  
110 counting of  $\phi$ Luz19 and  $\phi$ 14-1 densities in co-cultures. These resistant strains were derived  
111 by isolating colonies growing on high titre phage plaques and confirmed via sequencing [31].  
112 All monoculture and co-culture samples were quantified using the appropriate resistant  
113 strains to ensure consistency.

114

115

116 **Phage Separation and Concentration**

117 To generate high-titre and pure phage lysates for downstream assays and sequencing, we  
118 employed selective double-layer overlays with resistant hosts. Briefly, phages and φLUZ19-  
119 or φ14-1-resistant PAO1 strains were seeded into top agar plates to allow phage propagation.  
120 Phages were extracted from plates by scraping top-agar into 15ml falcon tubes containing  
121 5ml of phage buffer (NaCl (100 mM), MgSO<sub>4</sub> (10 mM), CaCl<sub>2</sub> (5 mM), Tris-HCl (pH 8) (50 mM),  
122 Gelatin (0.01%)). Tubes were mixed overnight after which phages were separated from top  
123 agar using sterile-filtration. This process was performed three times to ensure removal of  
124 phage competitors from co-culture populations. The purification and extraction protocols  
125 were identical to those described in ref. [31].

126 **Phage Growth Rate Assays**

127 The thermal phenotypes of purified evolved phage populations relative to the ancestor was  
128 assessed by measuring phage and bacterial growth across an 8h window under static  
129 incubation at 37°C and 42°C. Phage lysates were diluted to 10<sup>5</sup> PFU/ml and 300uL was mixed  
130 with 2.7ml of 10<sup>8</sup> CFU/ml wild-type PAO1 to a final MOI = ~0.0001. φLUZ19 was sampled at  
131 2h, 4h, and 8h; φ14-1 at 4h and 8h due to delayed replication. Phage quantification was  
132 performed through sterile-filtration through 0.22μm filter plates (Agilent) followed by  
133 centrifugation at 2,230xg for 5 mins before spotting onto resistant PAO1 double-layer overlay  
134 plates. Each growth rate assay included a single replicate of each evolved phage population  
135 and three replicates of the phage ancestor. Growth rate assays were repeated three times  
136 across a two-week period to produce three technical replicates.

137 **Phage Population Genomics**

138 **DNA Extraction and Sequencing**

139 Phage DNA was extracted from purified lysates as described in [31]. Briefly, ancestral and  
140 evolved phage lysates were treated with DNase and RNase to remove bacterial DNA and RNA.  
141 Phage particles were lysed using lysis (AL) buffer and proteinase K. Cell debris was  
142 precipitated using precipitation (N4) buffer and removed. Finally, DNA was precipitated and  
143 washed using isopropanol and ethanol. DNA quality was assessed with NanoDrop 2000c  
144 (Thermo Scientific) and quantified with Qubit 4 (Thermofisher). Short-read Illumina  
145 sequencing was performed by AZENTA/GENEWIZ using their Microbe-EZ pipeline for evolved  
146 and ancestral populations. Bacterial genomes (wild-type and phage-resistant strains) were  
147 sequenced by MicrobesNG using hybrid (long- and short-read) approaches.

148 **Sequence Analysis**

149 Phage reads were pre-processed with Trim Galore (v.0.5.0)  
150 (<https://github.com/FelixKrueger/TrimGalore>) and downsampled using bbnorm from the  
151 bbmap package (v.39.18) (<https://sourceforge.net/projects/bbmap/>). Reads were then  
152 mapped to de novo ancestral assemblies generated with shovill (v1.1.0)  
153 (<https://github.com/tseemann/shovill>) using Bowtie2 (v.2.3.4.2) [34]. Variants were  
154 identified using breseq (v.0.36.1) [35]. Ancestral assemblies were annotated with prokka

155 (v.1.14.5) [36], guided by the NCBI GenBank file for each phage ( $\phi$ 14-1: NC\_011703;  $\phi$ Luz19:  
156 NC\_010326).

157 Wild-type and resistant PAO1 genomes were assembled using Autocycler (v. 0.4.0) [37] and  
158 polished via Polypolish (v. 0.6.0) [38]. Final assemblies were re-oriented with Dnaapler (v.  
159 1.2.0) [39] and annotated using prokka (v.1.14.5) [36]. The workflow was deployed using a  
160 Dockerised Nextflow pipeline (v. 1.0.2) available  
161 at <https://doi.org/10.5281/zenodo.15706447>. Mutations in resistant PAO1 strains were  
162 identified by mapping long reads to the wild-type assembly with minimap2 (v.2.24) [40] and  
163 variant calling with medaka (v.2.1) (<https://github.com/nanoporetech/medaka>). All  
164 bioinformatic analyses were conducted with default parameters.

## 165 Statistical Analyses and Visualisation

166 All statistical analyses and data visualisation were conducted using packages in R (v.4.3.2) and  
167 RStudio [41,42]. Data wrangling was performed using “Tidyverse” (v.2.0.0) R packages [43].  
168 Phage growth and evolution rates were compared between evolution treatments using linear  
169 mixed effect models with the “lme4” (v.1.1-36) R package [44] where the response variable  
170 was phage density (pfu/ml) or genetic distance from ancestor, the explanatory variables were  
171 an interaction term between evolution treatment and temperature, and batch was a random  
172 effect. Within-group variation in genetic distance from ancestor was analysed using Levene’s  
173 test. The prevalence of unique compared to shared mutations across evolution treatments  
174 was analysed using Fisher’s exact test. Phage genetic distance between groups was also  
175 compared by constructing neighbour-joining trees based on Euclidean genetic distance using  
176 the “ggtree” (v.3.10.1) R package [45]. Data and code used in analyses can be found at  
177 [https://github.com/SamuelGreenrod/Evol\\_fluctuating](https://github.com/SamuelGreenrod/Evol_fluctuating).

178

## 179 Results

### 180 Fluctuating temperatures select for generalist phenotypes in monoculture

181 Fluctuating environments can favour generalists with intermediate phenotypes across  
182 conditions [1]. Given  $\phi$ 14-1 has previously been shown to grow poorly at 42°C, we  
183 hypothesised that  $\phi$ 14-1 populations passaged under fluctuating conditions would rapidly  
184 adapt to 42°C but have lower fitness at 37°C and 42°C compared to static evolved populations.  
185 In monoculture,  $\phi$ 14-1 densities increased during 37°C passages but decreased in 42°C  
186 passages (Fig. 1A). As phage lysates were diluted 10-fold in between passages, phage density  
187 decreases reflect lower than 10-fold  $\phi$ 14-1 population growth during 42°C passages.  $\phi$ Luz19  
188 monoculture populations reached and then maintained high densities in all passages. This  
189 phage showed low variation in inter-passage densities.

190 We assessed phage evolution by measuring the growth rates of static and fluctuating evolved  
191 populations relative to the ancestral phage through growth assays at 37°C and 42°C (Fig. 1B).  
192 We found that growth rates of both phages in monoculture depended on the interaction  
193 between evolution treatment and assay temperature ( $\phi$ 14-1:  $F_{3,29} = 125.8$ ,  $p < 0.001$ ;  $\phi$ Luz19:

194  $F_{3,29} = 96.0$ ,  $p < 0.001$ ). At 42°C,  $\phi$ 14-1 fluctuating populations were found to have an  
195 intermediate phenotype between those evolved under static conditions.  $\phi$ 14-1 fluctuating  
196 populations had significantly higher growth rates at 42°C than 37°C static populations ( $t(29)$   
197 = -12.4,  $p < 0.001$ ) but lower growth rates than 42°C static populations ( $t(29) = 12.7$ ,  $p < 0.001$ ).  
198 At 37°C,  $\phi$ 14-1 fluctuating populations had no significant difference to static populations  
199 possibly due to phage growth being measured after phages had reached carrying capacity  
200 (see ref. [31]). For  $\phi$ Luz19, fluctuating evolved populations had significantly higher growth at  
201 42°C than 37°C static populations ( $t(29) = -19.3$ ,  $p < 0.001$ ). However, growth was not  
202 significantly different to 42°C evolved populations ( $t(29) = -1.65$ ,  $p = 0.37$ ). The opposite  
203 findings were observed at 37°C; fluctuating evolved populations had significantly higher  
204 growth rates than those evolved at 42°C but similar growth rates to 37°C evolved populations  
205 (42°C static:  $t(29) = -5.2$ ,  $p < 0.001$ ; 37°C static:  $t(29) = -0.99$ ,  $p = 0.75$ ).

206

## 207 **Co-selection from fluctuating temperatures and competition constrains thermal adaptation**

208 The presence of additional selection pressures is expected to constrain adaptation to  
209 fluctuating temperatures by reducing mutational supply and compounding fitness trade-offs  
210 [12,18,19]. We hypothesised that phages evolved under co-selection from fluctuating  
211 temperatures and competition would have lower growth rates at 37°C and 42°C than those  
212 evolved under static temperatures or fluctuating monoculture conditions. While  $\phi$ 14-1  
213 densities fluctuated between passages in monoculture, co-culture densities rapidly increased  
214 and then stabilised between passages (Fig. 1A). In contrast,  $\phi$ Luz19 populations were stable  
215 in monoculture, but during fluctuations in co-culture, experienced high growth at 37°C and  
216 low growth at 42°C.

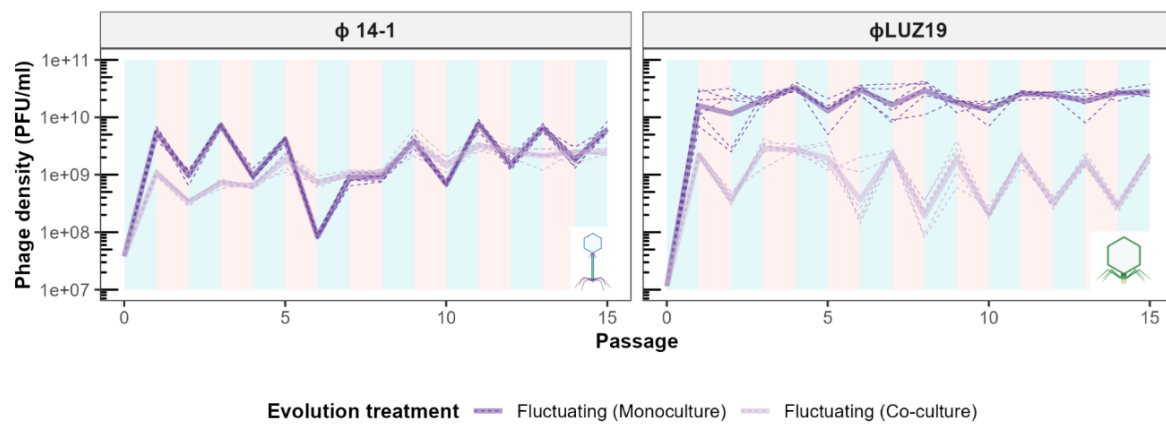
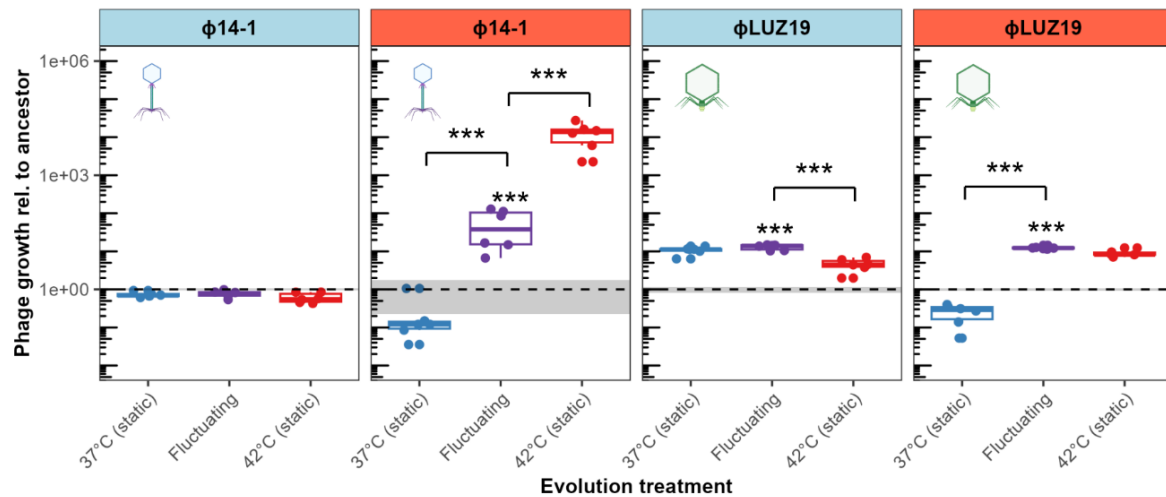
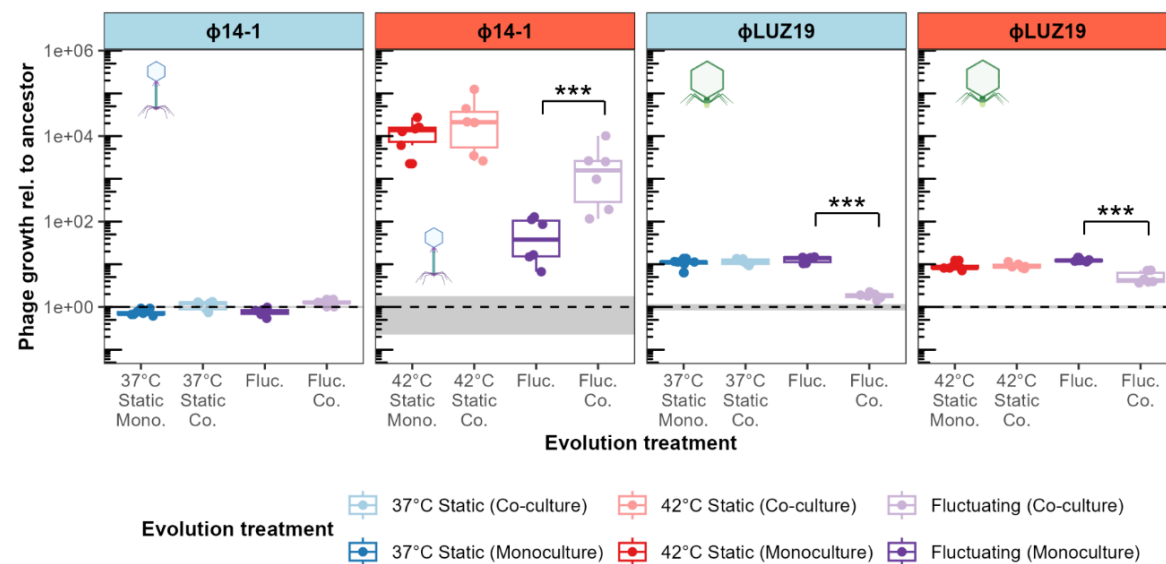
217 We then assessed evolved phage growth rates at 37°C and 42°C (Fig. 1C). We found a  
218 significant interaction between evolution treatment (monoculture and co-culture) and  
219 temperature regarding growth rates for both phages ( $\phi$ 14-1:  $F_{6,59} = 75.0$ ,  $p < 0.0001$ ;  $\phi$ Luz19:  
220  $F_{6,59} = 103.5$ ,  $p < 0.0001$ ). While competition had no impact on the growth rates of static  $\phi$ 14-  
221 1 populations (37°C:  $t(59) = -0.78$ ,  $p = 0.99$ ; 42°C:  $t(59) = -0.98$ ,  $p = 0.99$ ), fluctuating co-culture  
222 evolved populations had significantly higher growth rates at 42°C compared to populations  
223 evolved in monoculture ( $t(59) = -6.7$ ,  $p < 0.0001$ ). No significant difference was observed at  
224 37°C ( $t(59) = -1.0$ ,  $p = 0.99$ ). Similar to  $\phi$ 14-1, there was no impact of competition on static  
225 evolved  $\phi$ Luz19 population growth rates (37°C:  $t(59) = -0.42$ ,  $p = 1.0$ ; 42°C:  $t(59) = -0.21$ ,  $p =$   
226 1.0). However,  $\phi$ Luz19 populations evolved with fluctuations and competition had  
227 significantly lower growth rates at both 37°C and 42°C compared to monoculture (37°C:  $t(59)$   
228 = 10.1,  $p < 0.0001$ ; 42°C:  $t(59) = 4.9$ ,  $p < 0.001$ ).

229

230

231

232

**A****B****C**

234 **Figure 1. Co-selection in communities constrains adaptation to thermal fluctuations. A)**  
235 Population dynamics of phages passaged in monoculture and co-culture under fluctuating  
236 temperatures. Values show densities at the end of each passage prior to dilution. As phage  
237 lysates were diluted 10-fold in between passages, density decreases reflect less than 10-fold  
238 population growth during passages. Plot background colour reflects the temperature during  
239 that passage where light blue is 37°C and light red is 42°C. Phage icons illustrate the two  
240 different phages used in the experiments ( $\phi$ 14-1, myovirus in blue;  $\phi$ LUZ19, autographivirus  
241 in green) [46] and are used hereafter to refer to phages in figures. **B)** Fluctuating and static  
242 temperature evolved population growth rates relative to the ancestor. Growth rates were  
243 measured after 2h for  $\phi$ LUZ19 and 4h for  $\phi$ 14-1. Six biological replicates were assayed, and  
244 data points show the average of three technical replicates. Panel strip colour reflects the  
245 temperature that growth was tested at where light blue is 37°C and light red is 42°C.  
246 Fluctuating populations are presented in purple with 37°C static populations in blue and 42°C  
247 static populations in red. Ancestral growth is shown by dashed grey line with standard errors  
248 shown as a grey box ( $n = 3$ ). \*\*\* =  $p < 0.001$ . Absence of asterisk reflects non-significance.  
249 Static monoculture temperature data was adapted from ref. [31]. **C)** Growth rates of  
250 fluctuating and static temperature monoculture evolved populations compared to co-culture  
251 evolved populations. Boxes are coloured by evolution treatment with monoculture in dark  
252 (37°C static in blue, 42°C static in red, and fluctuating in purple) and co-culture in light (37°C  
253 static in light blue, 42°C static in light red, and fluctuating in light purple). Assay temperature  
254 and significance values are presented as in Fig. 1B. Six biological replicates were assayed and  
255 data points show the average of three technical replicates. Ancestral growth rates and  
256 significance signs are presented as in Fig. 1B. Static co-culture data was adapted from ref.  
257 [31].

258

259

## 260 **Fluctuating environments favour specialist mutations**

261 Fluctuating temperatures generally select for multiple specialist mutations [4]. We  
262 hypothesised that fluctuating evolved populations would show genetic similarities to both  
263 high and low temperature static populations. Phage genomic evolution was assessed by  
264 constructing neighbour-joining trees of end-point populations based on Euclidean genetic  
265 distances (Fig. 2A). Genetic distances were calculated based on the presence and frequency  
266 of genetic variants (SNPs, indels) that had  $> 10\%$  frequency. Fluctuating evolved populations  
267 did not form a unique clade but instead were found to co-locate with either high or low  
268 temperature static populations.  $\phi$ 14-1 fluctuating populations were distributed across the  
269 tree and generally did not cluster with static populations. Conversely,  $\phi$ LUZ19 fluctuating  
270 populations were primarily found within the 42°C static clade.

271 We further analysed static and fluctuating population genetic similarities by measuring  
272 evolution rates based on Euclidean genetic distance from ancestor (Fig. 2B). For  $\phi$ 14-1,  
273 fluctuating evolved populations had significantly lower evolution rates than 42°C static  
274 populations ( $t(15) = -4.1$ ,  $p < 0.01$ ). However, evolution rates were equal between fluctuating

275 and 37°C static populations ( $t(15) = -0.51$ ,  $p = 0.87$ ). There was no significant difference in  
276 evolution rates between  $\phi$ Luz19 fluctuating populations and either 37°C or 42°C static  
277 populations (37°C:  $t(15) = -0.46$ ,  $p = 0.89$ ; 42°C:  $t(15) = -0.75$ ,  $p = 0.74$ ). Notably,  $\phi$ 14-1  
278 fluctuating populations had significantly greater within-group variation in evolution rates  
279 compared to 42°C static populations ( $t(15) = 2.9$ ,  $p < 0.05$ ) but not 37°C static populations  
280 ( $t(15) = -0.70$ ,  $p = 0.77$ ).  $\phi$ Luz19 fluctuating populations had no significant difference in  
281 within-group variation compared to static populations (37°C:  $t(15) = 2.0$ ,  $p = 0.15$ ; 42°C:  $t(15)$   
282 =  $-0.10$ ,  $p = 0.99$ ).

283 We then determined the prevalence of individual genetic variants (SNPs, indels) that were  
284 unique to or shared between evolution treatments (Fig. 2C). Only putative adaptive variants  
285 with >20% frequency were included. For  $\phi$ 14-1, 2/11 (18%) of 37°C static variants and 5/15  
286 (33%) of 42°C static variants were shared with other evolution treatments compared to 4/9  
287 (44%) variants in fluctuating evolved populations. For  $\phi$ Luz19, shared variants constituted  
288 8/32 (35%) of 37°C static and 9/20 (45%) of 42°C static variants compared to 12/17 (71%) in  
289 fluctuating evolved populations. To assess the overall impact of evolution treatment on the  
290 ratio of unique and shared mutations, we pooled mutations from  $\phi$ 14-1 and  $\phi$ Luz19  
291 observing a significant difference in the prevalence of shared mutations relative to unique  
292 mutations between evolution treatments (Fisher's exact test:  $p < 0.05$ ). Significant differences  
293 were not observed when analysing phages independently ( $\phi$ 14-1,  $p = 0.47$ ;  $\phi$ Luz19,  $p = 0.08$ ).  
294  $\phi$ 14-1 fluctuating mutations were primarily shared with 42°C static populations (Fig. S1). In  
295 contrast,  $\phi$ Luz19 fluctuating mutations were shared equally with 37°C and 42°C static  
296 populations.

297 Finally, we investigated which mutations drove clustering between fluctuating and static  
298 populations (Fig. S2; Table S1). While  $\phi$ 14-1 fluctuating and 37°C static populations showed  
299 little clustering, two fluctuating populations clustered with the 42°C static clade. These two  
300 replicate populations contained parallel deletions in a hypothetical protein with high  
301 similarity to a DNA ligase (BlastP: 97.47% identity, 95% sequence overlap with *Pseudomonas*  
302 phage PhL\_UNISO\_PA-DSM\_ph0031 DNA ligase protein), previously identified in all  $\phi$ 14-1  
303 42°C static populations [31]. The clustering of 5/6  $\phi$ Luz19 fluctuating populations with the  
304 42°C static populations were attributed to parallel insertions in an intergenic region between  
305 two hypothetical proteins. This intergenic insertion was also previously identified in all  
306  $\phi$ Luz19 42°C static populations [31].

307

308

309

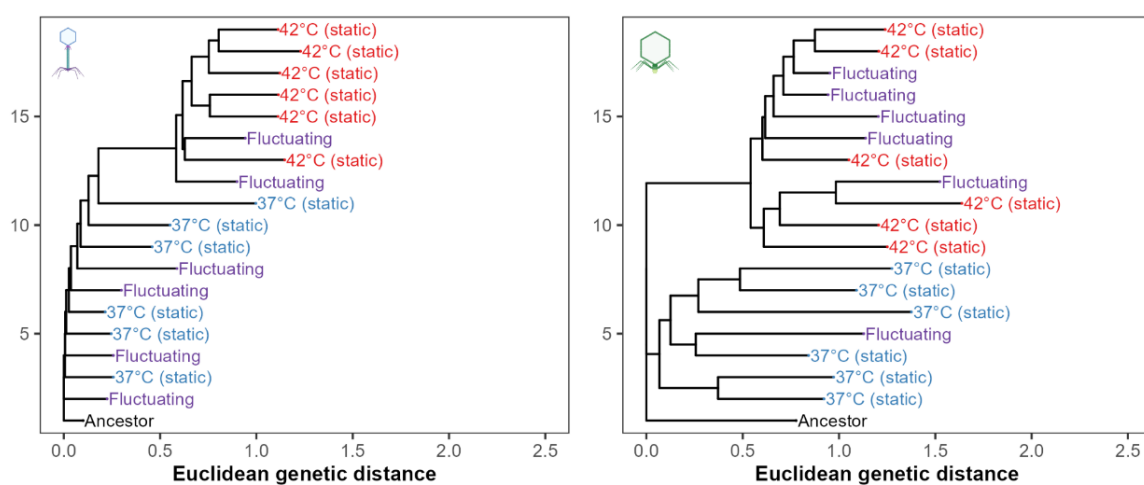
310

311

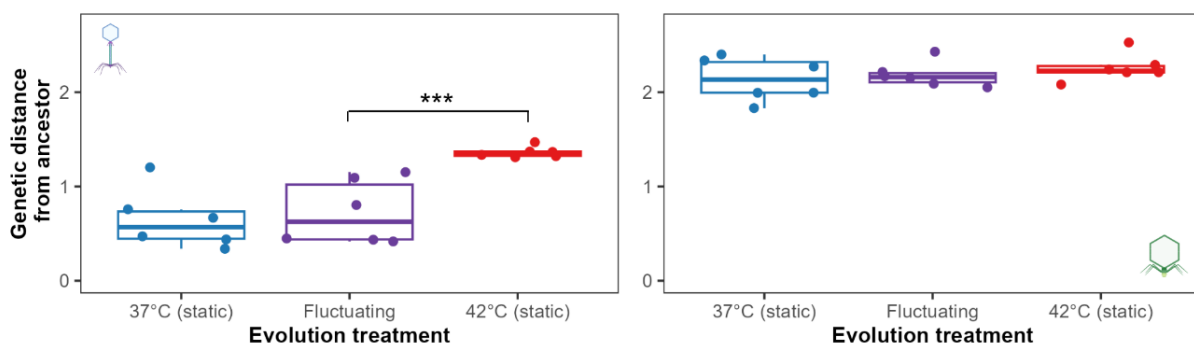
312

313

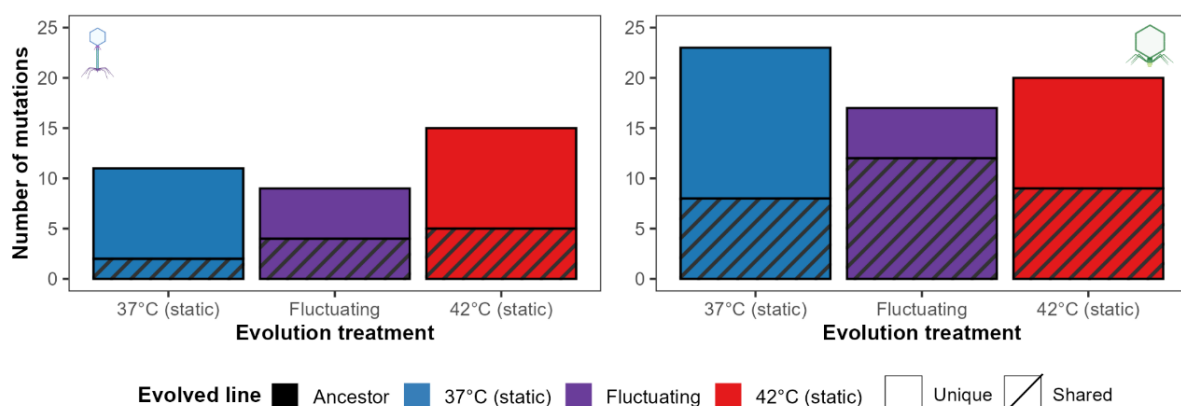
A



B



C



314

315 **Figure 2. Fluctuating temperatures select for specialist mutations.** A) Neighbour-joining  
 316 trees of evolved and ancestral phage populations constructed using Euclidean genetic  
 317 distances. Genetic distances were calculated based on the presence and frequency of  
 318 mutations present at > 10% frequency. Tree is rooted at the ancestor and populations are  
 319 coloured by evolved treatment. B) Phage evolution rates, measured based on Euclidean  
 320 genetic distance from the ancestor, for evolved monoculture phage populations. \*\*\* = p <  
 321 0.001. C) Stacked bar charts show the number of high frequency (>20% frequency), putative

322 adaptive variants that are unique to or shared between evolution treatments. Bars are  
323 coloured by evolution treatment. Unique genes are shown as clear bars and shared genes are  
324 shown as striped bars. Static temperature data was adapted from ref. [31].

325

### 326 **Co-selection constrains molecular evolution**

327 By reducing growth rates, co-selection from fluctuating temperatures and competition are  
328 expected to reduce evolution rates and restrict the acquisition of adaptive mutations [12].  
329 Due to their elevated growth rates, we hypothesised that  $\phi$ 14-1 fluctuating co-culture  
330 populations would have higher evolution rates than monoculture populations. No significant  
331 difference in evolution rate was observed for  $\phi$ 14-1 co-culture populations compared to  
332 monoculture populations ( $F_{1,10} = 4.1$ ,  $p = 0.07$ ) (Fig. 3A). However, non-significance was driven  
333 by a single low evolution rate replicate in the co-culture treatment; when the replicate was  
334 removed, co-culture populations had significantly greater evolution rates than monoculture  
335 ( $F_{1,9} = 8.6$ ,  $p < 0.05$ ). We also found no significant difference in within-group variation in  
336 evolution rates between monoculture and co-culture populations ( $t(10) = 1.50$ ,  $p = 0.17$ ),  
337 although the difference was also significant once the low evolution rate co-culture replicate  
338 was removed ( $t(10) = 3.6$ ,  $p < 0.01$ ).

339 For  $\phi$ Luz19, we hypothesised that fluctuating co-culture populations would have lower  
340 evolution rates than monoculture populations due to the suppression of  $\phi$ Luz19 by  $\phi$ 14-1.  
341  $\phi$ Luz19 fluctuating co-culture populations had significantly lower evolution rates than  
342 monoculture populations ( $F_{1,10} = 470$ ,  $p < 0.001$ ). We further hypothesised that  $\phi$ Luz19  
343 fluctuating co-culture populations, but not  $\phi$ 14-1 populations, would have lower evolution  
344 rates than 37°C or 42°C static co-culture populations. Evolution rates were equal between co-  
345 culture populations for  $\phi$ 14-1 ( $F_{2,15} = 1.2$ ,  $p = 0.3$ ) (Fig. 3B). However,  $\phi$ Luz19 fluctuating co-  
346 culture populations were found to have significantly lower evolution rates than both 37°C  
347 static and 42°C static monoculture populations (37°C:  $t(15) = 4.5$ ,  $p < 0.01$ ; 42°C:  $t(30) = 3.0$ ,  $p$   
348 < 0.05).

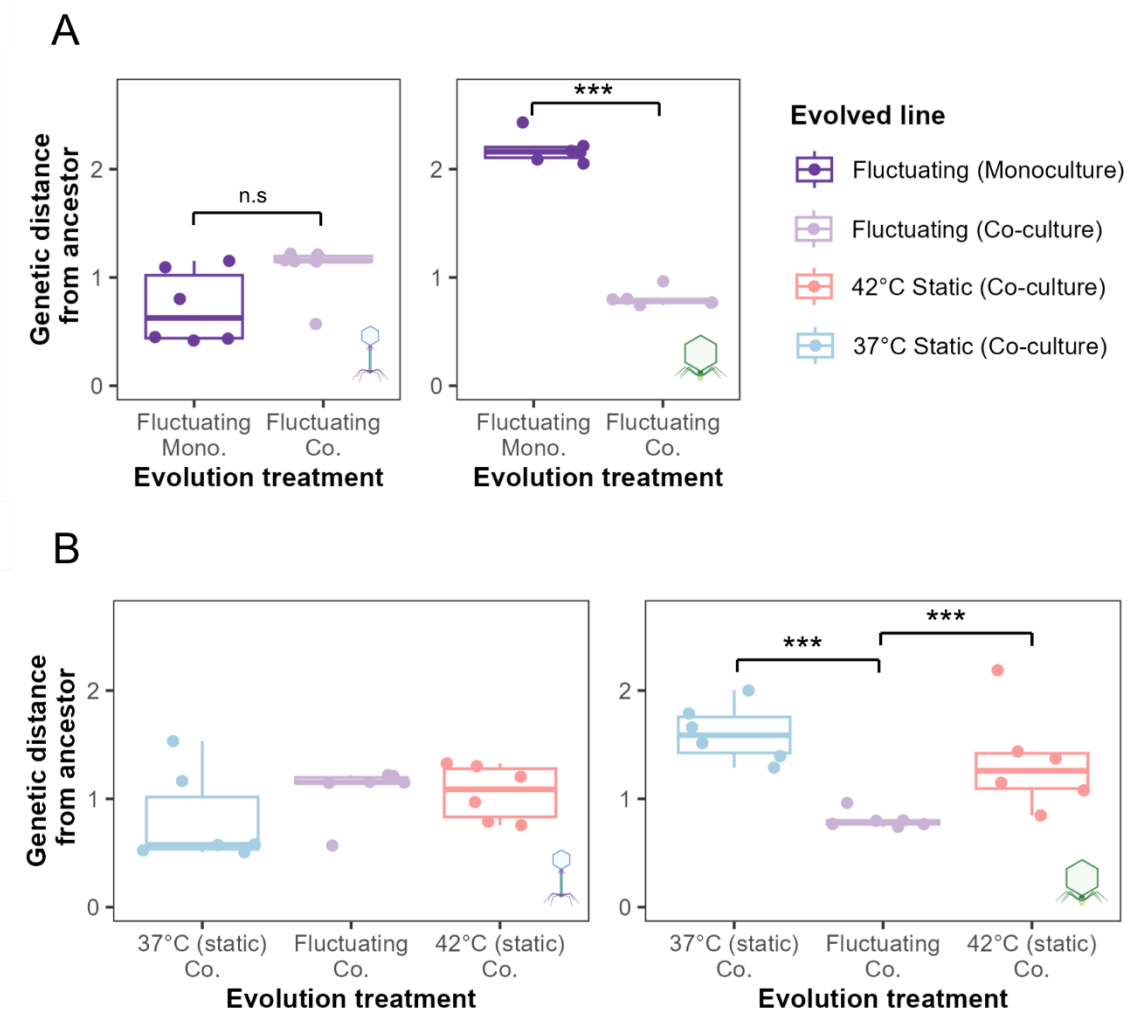
349 Finally, we assessed the impact of competition on the acquisition of high frequency mutations  
350 (> 20% frequency) in fluctuating populations (Fig. S3). For  $\phi$ 14-1, while populations no longer  
351 acquired singleton mutations, all populations acquired a deletion or SNP in a putative DNA  
352 ligase gene. Mutations in this gene are thought to contribute to high temperature adaptation  
353 [31] and were also found in the two monoculture populations which clustered with 42°C static  
354 populations in Fig. 2A. For  $\phi$ Luz19, while co-culture populations maintained mutations in tail  
355 fiber genes, the populations no longer acquired singleton mutations or the intergenic  
356 insertion associated with 42°C static populations.

357

358

359

360



361

362 **Figure 3. High environmental complexity constrains evolution rates.** A) Evolution rates,  
363 measured based on Euclidean genetic distance from the ancestor, of phage populations  
364 evolved under fluctuating temperatures in monoculture (deep purple) and co-culture (light  
365 purple). B) Evolution rates of 37°C static, fluctuating, and 42°C static co-culture populations.  
366 Plot layout is the same as panel A. \*\*\* = p < 0.001. N.S is used to denote lack of statistical  
367 significance. Static temperature data was adapted from ref. [31].

368

## 369 Discussion

370 Under fluctuating selection, both phages were found to rapidly evolve increased growth rates  
371 at high temperatures. For phage  $\phi$ 14-1, fluctuating temperatures favoured intermediate  
372 thermal phenotypes with lower growth rates at high temperatures compared to phages  
373 evolved under static temperatures. The evolution of intermediate growth rates is likely due  
374 to weaker selection for adaptation to high temperatures in the fluctuating treatment.  
375 Alternatively, adaptation to high temperatures may be constrained during fluctuations due to  
376 fitness trade-offs at lower temperatures [47]. For phage  $\phi$ Luz19, fluctuating temperature  
377 populations had the same growth rates as static-evolved populations when measured at their

378 evolved temperature. Given  $\phi$ Luz19 was shown to exhibit growth rate trade-offs under static  
379 selection [31], this finding is indicative of a no-cost generalist strategy [48]. The lack of growth  
380 rate costs may reflect an epistatic pleiotropy, whereby the costs of adaptive mutations  
381 depend on the genetic background [48]. Costs may also occur in unmeasured traits such as  
382 virulence [49] or tolerance to other stresses [15]. These findings highlight that, while  
383 fluctuating temperatures select for greater high temperature growth, the exact phenotypic  
384 outcomes of fluctuating selection vary between phage taxa [50].

385 We found that fluctuating temperatures resulted in more variable evolutionary trajectories;  
386 while static evolved populations generally formed clusters, fluctuating populations were  
387 genetically similar to both 37°C and 42°C static evolved populations. Further, we found that  
388 parallel mutations acquired under fluctuating selection were the same as those previously  
389 identified in static evolved populations [31]. These findings could be explained by historical  
390 contingency [51] whereby random mutations that are adaptive at low or high temperatures  
391 become fixed in a subset of populations [7]. Depending on the timing of mutation appearance,  
392 fluctuating populations may then resemble individual static environments. Fluctuating  
393 environments have also been shown to select for mutations conferring fitness in the most  
394 extreme environment [52]. The clustering of  $\phi$ Luz19 fluctuating populations with 42°C static  
395 populations likely reflects selective sweeps combined with asymmetrical selection where  
396 42°C adaptive variants are fixed more rapidly.

397 While fluctuating environments can promote genetic diversification, co-selection with other  
398 environmental stressors can constrain adaptation [12]. Uiterwaal et al [18] showed that  
399 combined fluctuating temperatures and predation restricted adaptation to both selection  
400 pressures in *Paramecium caudatum* populations. Similar findings have also been observed in  
401 *Daphnia magna* with co-selection from thermal fluctuations and predation/pollutants  
402 [19,53]. We found that combined fluctuating temperature- and competition-based selection  
403 constrained both thermal adaptation and slowed evolutionary rates in phage  $\phi$ Luz19.  
404 Further, co-selection resulted in greater  $\phi$ Luz19 evolutionary constraint with fluctuating  
405 temperatures than static temperatures. The negative effects of combined environmental  
406 stressors are often non-additive and instead exhibit synergies [12]. We have previously shown  
407 that selection from high temperatures synergises with competition to constrain  $\phi$ Luz19  
408 evolution rates [31]. The present study extends these findings by showing that the selective  
409 synergy between temperature and competition is greater under fluctuating temperatures  
410 than static temperatures. One potential explanation for these findings is that fluctuating  
411 environments reduce the strength of selection for adaptive mutations [54]. Weaker  
412 directional selection combined with suppression by competitors may constrain both the  
413 supply and fixation of beneficial mutations leading to particularly low evolution rates.

414 Anthropogenic activities, including global climate change, mean that species are facing  
415 increasingly variable and complex environments [55]. With ongoing global biodiversity loss,  
416 species must adapt to tolerate environmental stressors to avoid extinctions. Our findings  
417 highlight that while species can rapidly adapt in response to thermal variation, co-selection  
418 with other stressors, such as competition, may restrict species adaptive capacity. These  
419 results have particular relevance for parasites which must simultaneously adapt to both

420 thermal heterogeneity, community competition in coinfections, and host immune responses.  
421 With global parasite biodiversity at risk due to climate change [26], evolutionary constraint  
422 caused by co-selection may prevent parasite adaptation to thermal stress and further  
423 increase the probability of parasite extinctions. Future studies should consider the evolution-  
424 constraining effects of co-selection when assessing species extinction risk in thermally  
425 variable environments.

426

## 427 **Acknowledgments**

428 We thank R. Salguero-Gomez, T. Richards, T. Barraclough, and K. Foster for feedback on the  
429 experimental design and results. This work was supported by the Biotechnology and  
430 Biosciences Research Council (BB/T008784/1) to S.T.E.G. as well as the Natural Environment  
431 Research Council (NE/X000540/1) and NSERC Canada Excellence Research Chair to K.C.K. The  
432 funders had no role in study design, data collection and interpretation, or the decision to  
433 submit the work for publication. Fluctuating evolved phage sequence reads are accessible on  
434 NCBI (<https://www.ncbi.nlm.nih.gov/>) under BioProject ID: PRJNA1334331. Static evolved  
435 phage sequence reads and bacterial sequence reads from ref. [31] are accessible under  
436 BioProject IDs: PRJNA1332698 and PRJNA1332799, respectively.

437

## 438 **References**

- 439 1. Kassen R. The experimental evolution of specialists, generalists, and the maintenance of  
440 diversity. *Journal of Evolutionary Biology*. 2002;15(2):173–90.
- 441 2. Sachdeva V, Husain K, Sheng J, Wang S, Murugan A. Tuning environmental timescales to evolve  
442 and maintain generalists. *Proceedings of the National Academy of Sciences*. 2020 Jun  
443 9;117(23):12693–9.
- 444 3. Kassen R, Bell G. Experimental evolution in Chlamydomonas. IV. Selection in environments that  
445 vary through time at different scales. *Heredity*. 1998;80(6):732–41.
- 446 4. Lambros M, Pechuan-Jorge X, Biro D, Ye K, Bergman A. Emerging Adaptive Strategies Under  
447 Temperature Fluctuations in a Laboratory Evolution Experiment of Escherichia Coli. *Front  
448 Microbiol*. 2021 Oct 22;12:724982.
- 449 5. Sandberg TE, Lloyd CJ, Palsson BO, Feist AM. Laboratory Evolution to Alternating Substrate  
450 Environments Yields Distinct Phenotypic and Genetic Adaptive Strategies. *Appl Environ  
451 Microbiol*. 2017 Jun 16;83(13):e00410-17.
- 452 6. Abdul-Rahman F, Tranchina D, Gresham D. Fluctuating Environments Maintain Genetic  
453 Diversity through Neutral Fitness Effects and Balancing Selection. *Molecular Biology and  
454 Evolution*. 2021 Oct 1;38(10):4362–75.
- 455 7. Harrison E, Laine AL, Hietala M, Brockhurst MA. Rapidly fluctuating environments constrain  
456 coevolutionary arms races by impeding selective sweeps. *Proc Biol Sci*. 2013 Aug  
457 7;280(1764):20130937.

- 458 8. Chesson P. Mechanisms of Maintenance of Species Diversity. *Annual Review of Ecology, Evolution, and Systematics*. 2000 Nov 1;31(Volume 31, 2000):343–66.
- 460 9. Gilchrist GW. Specialists and Generalists in Changing Environments. I. Fitness Landscapes of Thermal Sensitivity. *The American Naturalist*. 1995;146(2):252–70.
- 462 10. Gunderson AR, Armstrong EJ, Stillman JH. Multiple Stressors in a Changing World: The Need for an Improved Perspective on Physiological Responses to the Dynamic Marine Environment. *Annual Review of Marine Science*. 2016 Jan 3;8(Volume 8, 2016):357–78.
- 465 11. Hector TE, Hoang KL, Li J, King KC. Symbiosis and host responses to heating. *Trends in Ecology & Evolution*. 2022 Jul 1;37(7):611–24.
- 467 12. Crain CM, Kroeker K, Halpern BS. Interactive and cumulative effects of multiple human stressors in marine systems. *Ecology Letters*. 2008;11(12):1304–15.
- 469 13. Hiltunen T, Cairns J, Frickel J, Jalasvuori M, Laakso J, Kaitala V, et al. Dual-stressor selection alters eco-evolutionary dynamics in experimental communities. *Nat Ecol Evol*. 2018 Dec;2(12):1974–81.
- 472 14. Burmeister AR, Fortier A, Roush C, Lessing AJ, Bender RG, Barahman R, et al. Pleiotropy complicates a trade-off between phage resistance and antibiotic resistance. *Proceedings of the National Academy of Sciences*. 2020 May 26;117(21):11207–16.
- 475 15. Schou MF, Engelbrecht A, Brand Z, Svensson EI, Cloete S, Cornwallis CK. Evolutionary trade-offs between heat and cold tolerance limit responses to fluctuating climates. *Science Advances*. 2022 May 27;8(21):eabn9580.
- 478 16. Yamamichi M, Letten AD, Schreiber SJ. Eco-evolutionary maintenance of diversity in fluctuating environments. *Ecol Lett*. 2023 Sep;26 Suppl 1:S152–67.
- 480 17. Cairns J, Borse F, Mononen T, Hiltunen T, Mustonen V. Strong selective environments determine evolutionary outcome in time-dependent fitness seascapes. *Evol Lett*. 2022 Jun 1;6(3):266–79.
- 483 18. Uiterwaal SF, Lagerstrom IT, Luhring TM, Salsbery ME, DeLong JP. Trade-offs between morphology and thermal niches mediate adaptation in response to competing selective pressures. *Ecology and Evolution*. 2020;10(3):1368–77.
- 486 19. Barbosa M, Pestana J, Soares AMVM. Predation Life History Responses to Increased Temperature Variability. *PLoS One*. 2014 Sep 24;9(9):e107971.
- 488 20. Vinebrooke R, L. Cottingham K, Norberg J, Marten Scheffer, I. Dodson S, C. Maberly S, Sommer U. Impacts of multiple stressors on biodiversity and ecosystem functioning: the role of species co-tolerance. *Oikos*. 2004;104(3):451–7.
- 491 21. Halpern BS, Walbridge S, Selkoe KA, Kappel CV, Micheli F, D'Agrosa C, et al. A Global Map of Human Impact on Marine Ecosystems. *Science*. 2008 Feb 15;319(5865):948–52.
- 493 22. Bellard C, Bertelsmeier C, Leadley P, Thuiller W, Courchamp F. Impacts of climate change on the future of biodiversity. *Ecology Letters*. 2012;15(4):365–77.

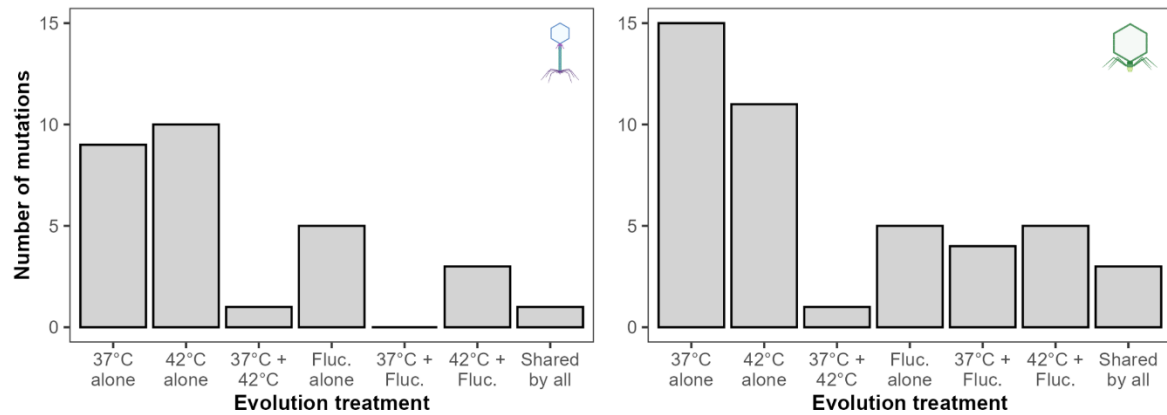
- 495 23. Nguyen PL, Gokhale CS. On multiple infections by parasites with complex life cycles. *Oikos*.  
496 2025;2025(4):e10493.
- 497 24. Silva LM, King KC, Koella JC. Dissecting transmission to understand parasite evolution. *PLoS*  
498 *Pathog.* 2025 Mar 25;21(3):e1012964.
- 499 25. Oakley MS, Gerald N, McCutchan TF, Aravind L, Kumar S. Clinical and molecular aspects of  
500 malaria fever. *Trends in Parasitology*. 2011 Oct 1;27(10):442–9.
- 501 26. Carlson CJ, Burgio KR, Dougherty ER, Phillips AJ, Bueno VM, Clements CF, et al. Parasite  
502 biodiversity faces extinction and redistribution in a changing climate. *Science Advances*. 2017  
503 Sep 6;3(9):e1602422.
- 504 27. Buckingham LJ, Ashby B. Coevolutionary theory of hosts and parasites. *j evol Biol.* 2022 Feb  
505 1;35(2):205–24.
- 506 28. Pedersen AB, Fenton A. Emphasizing the ecology in parasite community ecology. *Trends in*  
507 *Ecology & Evolution*. 2007 Mar 1;22(3):133–9.
- 508 29. Hasik AZ, King KC, Hawlena H. Interspecific host competition and parasite virulence evolution.  
509 *Biology Letters*. 2023 May 3;19(5):20220553.
- 510 30. Limberger R, Fussmann GF. Adaptation and competition in deteriorating environments.  
511 *Proceedings of the Royal Society B: Biological Sciences*. 2021 Mar 10;288(1946):20202967.
- 512 31. Greenrod ST, Cazares D, Slesak WA, Hector T, MacLean RC, King KC. Evolutionary rescue  
513 accelerates competitive exclusion in a parasite community [Internet]. *bioRxiv*; 2025 [cited 2025  
514 Sep 28]. p. 2025.09.25.678511. Available from:  
515 <https://www.biorxiv.org/content/10.1101/2025.09.25.678511v1>
- 516 32. Greenrod STE, Cazares D, Johnson S, Hector TE, Stevens EJ, MacLean RC, et al. Warming alters  
517 life-history traits and competition in a phage community. *Applied and Environmental*  
518 *Microbiology*. 2024 Apr 16;0(0):e00286-24.
- 519 33. Kropinski AM, Mazzocco A, Waddell TE, Lingohr E, Johnson RP. Enumeration of Bacteriophages  
520 by Double Agar Overlay Plaque Assay. In: Clokie MRJ, Kropinski AM, editors. *Bacteriophages: Methods and Protocols, Volume 1: Isolation, Characterization, and Interactions* [Internet].  
521 Totowa, NJ: Humana Press; 2009 [cited 2023 Jun 2]. p. 69–76. (Methods in Molecular  
522 Biology™). Available from: [https://doi.org/10.1007/978-1-60327-164-6\\_7](https://doi.org/10.1007/978-1-60327-164-6_7)
- 524 34. Langmead B, Salzberg SL. Fast gapped-read alignment with Bowtie 2. *Nat Methods*. 2012  
525 Apr;9(4):357–9.
- 526 35. Deatherage DE, Barrick JE. Identification of mutations in laboratory evolved microbes from  
527 next-generation sequencing data using breseq. *Methods Mol Biol.* 2014;1151:165–88.
- 528 36. Seemann T. Prokka: rapid prokaryotic genome annotation. *Bioinformatics*. 2014 Jul  
529 15;30(14):2068–9.
- 530 37. Wick RR, Howden BP, Stinear TP. Autocycler: long-read consensus assembly for bacterial  
531 genomes [Internet]. *bioRxiv*; 2025 [cited 2025 Jul 29]. p. 2025.05.12.653612. Available from:  
532 <https://www.biorxiv.org/content/10.1101/2025.05.12.653612v1>

- 533 38. Wick RR, Holt KE. Polypolish: Short-read polishing of long-read bacterial genome assemblies.  
534 PLOS Computational Biology. 2022 Jan 24;18(1):e1009802.
- 535 39. Bouras G, Grigson SR, Papudeshi B, Mallawaarachchi V, Roach MJ. Dnaapler: A tool to reorient  
536 circular microbial genomes. Journal of Open Source Software. 2024 Jan 11;9(93):5968.
- 537 40. Li H. Minimap2: pairwise alignment for nucleotide sequences. Bioinformatics. 2018 Sep  
538 15;34(18):3094–100.
- 539 41. RStudio Team. RStudio: Integrated Development for R. [Internet]. RStudio, PBC, Boston, M;  
540 2020. Available from: <http://www.rstudio.com/>
- 541 42. R Core Team. R: A language and environment for statistical computing. [Internet]. Foundation  
542 for Statistical Computing, Vienna, Austria.; 2021. Available from: <https://www.R-project.org/>
- 543 43. Wickham H, Averick M, Bryan J, Chang W, McGowan LD, François R, et al. Welcome to the  
544 Tidyverse. Journal of Open Source Software. 2019 Nov 21;4(43):1686.
- 545 44. Bates D, Mächler M, Bolker B, Walker S. Fitting Linear Mixed-Effects Models Using lme4.  
546 Journal of Statistical Software. 2015 Oct 7;67:1–48.
- 547 45. Yu G, Smith DK, Zhu H, Guan Y, Lam TTY. ggtree: an r package for visualization and annotation  
548 of phylogenetic trees with their covariates and other associated data. Methods in Ecology and  
549 Evolution. 2017;8(1):28–36.
- 550 46. Tabare E, Glonti T, Cochez C, Ngassam C, Pirnay JP, Amighi K, et al. A Design of Experiment  
551 Approach to Optimize Spray-Dried Powders Containing *Pseudomonas aeruginosa*Podoviridae  
552 and Myoviridae Bacteriophages. Viruses. 2021 Oct;13(10):1926.
- 553 47. Visher E, Boots M. The problem of mediocre generalists: population genetics and eco-  
554 evolutionary perspectives on host breadth evolution in pathogens. Proc Biol Sci. 2020 Aug  
555 26;287(1933):20201230.
- 556 48. Remold S. Understanding specialism when the jack of all trades can be the master of all.  
557 Proceedings of the Royal Society B: Biological Sciences. 2012 Oct 24;279(1749):4861–9.
- 558 49. Ashrafi R, Bruneaux M, Sundberg LR, Pulkkinen K, Valkonen J, Ketola T. Broad thermal  
559 tolerance is negatively correlated with virulence in an opportunistic bacterial pathogen.  
560 Evolutionary Applications. 2018;11(9):1700–14.
- 561 50. Wolinska J, King KC. Environment can alter selection in host–parasite interactions. Trends in  
562 Parasitology. 2009 May 1;25(5):236–44.
- 563 51. Blount ZD, Lenski RE, Losos JB. Contingency and determinism in evolution: Replaying life’s tape.  
564 Science. 2018 Nov 9;362(6415):eaam5979.
- 565 52. Arribas M, Kubota K, Cabanillas L, Lázaro E. Adaptation to Fluctuating Temperatures in an RNA  
566 Virus Is Driven by the Most Stringent Selective Pressure. PLOS ONE. 2014 Jun 25;9(6):e100940.
- 567 53. Barbosa M, Inocentes N, Soares AMVM, Oliveira M. Synergy effects of fluoxetine and variability  
568 in temperature lead to proportionally greater fitness costs in *Daphnia*: A multigenerational  
569 test. Aquatic Toxicology. 2017 Dec 1;193:268–75.

- 570 54. Cvijović I, Good BH, Jerison ER, Desai MM. Fate of a mutation in a fluctuating environment.  
571 Proc Natl Acad Sci U S A. 2015 Sep 8;112(36):E5021–8.
- 572 55. Jaureguiberry P, Titeux N, Wiemers M, Bowler DE, Coscione L, Golden AS, et al. The direct  
573 drivers of recent global anthropogenic biodiversity loss. Science Advances. 2022 Nov  
574 9;8(45):eabm9982.
- 575
- 576
- 577
- 578
- 579
- 580
- 581
- 582
- 583
- 584
- 585
- 586
- 587
- 588
- 589
- 590
- 591
- 592
- 593
- 594
- 595
- 596
- 597
- 598
- 599
- 600
- 601

602 **Extended data**

603



604

605 **Figure S1. Bar charts show the number of high frequency variants (> 20% frequency) that are unique**  
606 **to or shared between evolution treatments.** Variants are shown as either unique to individual

607 evolution treatments, shared between two treatments, or shared by all three. Static temperature data  
608 was adapted from ref. [31].

609

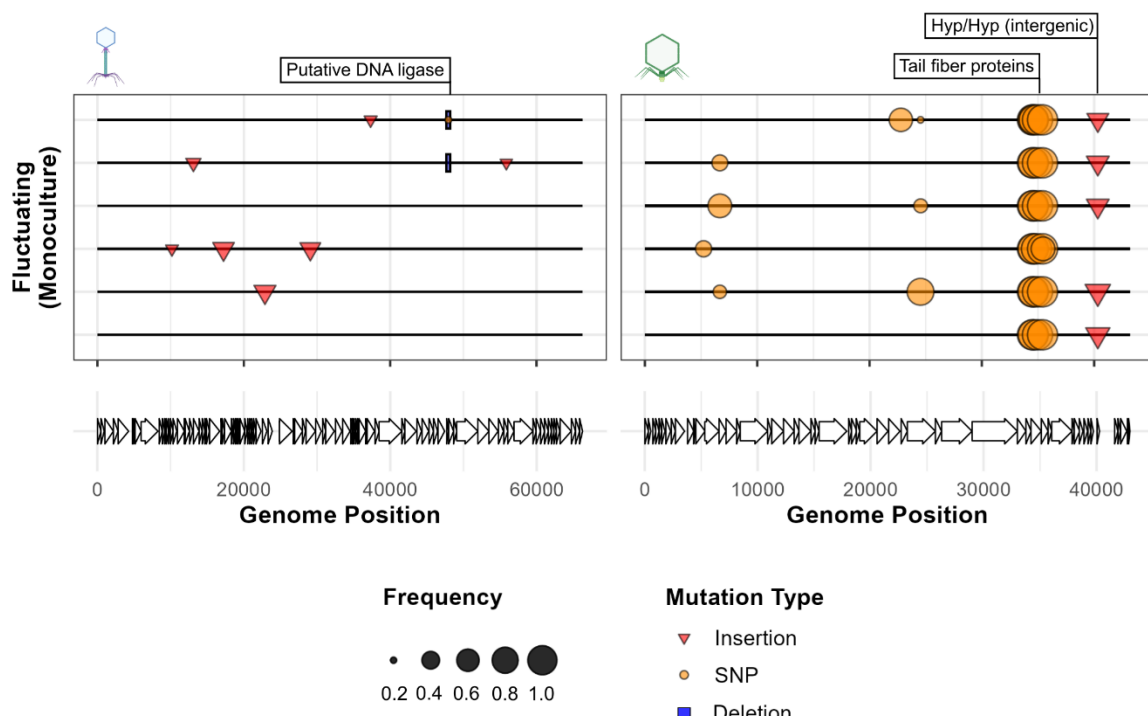
610

611

612

613

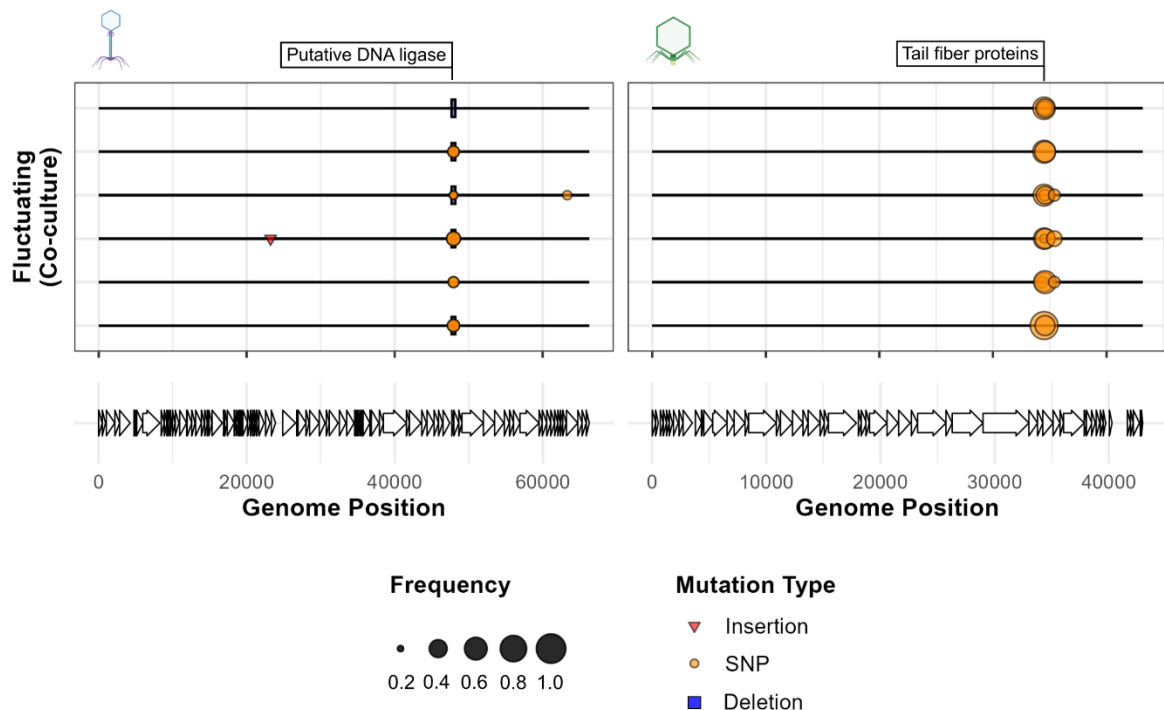
614



615

616 **Figure S2. Fluctuating temperatures select for specialist mutations.** Mutation plots show genetic  
 617 variants associated with fluctuating temperatures in monoculture in phage populations. Lines  
 618 represent individual biological replicates. Symbols within plots show variants across the phage  
 619 genome at > 20% prevalence and which were not observed in the ancestral population. Length of  
 620 deletion bars represent the size of deletion except for the  $\phi$ 14-1 deletion at ~48kb which is a 1bp  
 621 deletion but given a fixed size for visibility. Labels show gene annotations for mutations found in 37°C  
 622 and 42°C evolved populations [31]. Putative DNA ligase in  $\phi$ 14-1 was originally annotated a  
 623 hypothetical protein but has high homology to Pseudomonas phage PhL\_UNISO\_PA-DSM\_ph0031  
 624 DNA ligase protein.

625



626

627 **Figure S3. Competition restricts the acquisition of high frequency mutations.** Mutation plots show  
 628 genetic variants associated with fluctuating temperatures in co-culture in phage populations. Lines  
 629 represent individual biological replicates. Symbols within plots show variants across the phage  
 630 genome at > 20% prevalence and which were not observed in the ancestral population. Length of  
 631 deletion bars represent the size of deletion except for the  $\phi$ 14-1 deletion at ~48kb which is a 1bp  
 632 deletion but given a fixed size for visibility. Labels show gene annotations for mutations found in 37°C  
 633 and 42°C evolved populations [31]. Putative DNA ligase in  $\phi$ 14-1 was originally annotated a  
 634 hypothetical protein but has high homology to Pseudomonas phage PhL\_UNISO\_PA-DSM\_ph0031  
 635 DNA ligase protein.

636